Identification of Polymers as Major Components of Atmospheric Organic Aerosols

M. Kalberer,[1]* D. Paulsen,[2] M. Sax,[1] M. Steinbacher,[2] J. Dommen,[2] A. S. H. Prevot,[2] R. Fisseha,[2] E. Weingartner,[2] V. Frankevich,[1] R. Zenobi,[1] U. Baltensperger[2]*

Results from photooxidation of aromatic compounds in a reaction chamber show that a substantial fraction of the organic aerosol mass is composed of polymers. This polymerization results from reactions of carbonyls and their hydrates. After aging for more than 20 hours, about 50% of the particle mass consists of polymers with a molecular mass up to 1000 daltons. This results in a lower volatility of this secondary organic aerosol and a higher aerosol yield than a model using vapor pressures of individual organic species would predict.

Ambient aerosol particles contribute to many important atmospheric processes, including visibility reduction, cloud formation, direct radiative forcing, and also a variety of adverse health effects. Although organic material is a major fraction of ambient aerosol mass [often 20 to 50% (*1*)], only a minor fraction was identified so far on a molecular level (*2*). Up to 90% of the organic aerosol mass in urban areas is secondary organic aerosol (SOA) (*3*), which is not directly emitted but formed in the atmosphere by the oxidation of gaseous precursors. Small aromatic compounds such as benzene, toluene, xylenes, and trimethylbenzenes are the major known compounds emitted by human activities (mainly from fossil fuels), which lead to the formation of SOA.

Efforts have been made to quantify the aerosol formation potential (aerosol yield) of these aromatic compounds (*4*, *5*). Odum *et al.* showed that the aerosol yield of whole gasoline vapor can be explained by the sum of the single SOA yields of its aromatic constituents (*6*). Models describing SOA formation assume a thermodynamic equilibrium of organic compounds between the gas and the aerosol phase (*4*, *7*). Although the physical mass formation of SOA can be parameterized with established models (*4*, *8*, *9*), the chemical composition of the SOA is still poorly understood. The current methods of identification are mostly gas chromatography–mass spectrometry (GC-MS) along with infrared spectroscopy (*4*, *10*–*12*). SOA compounds identified so far from aromatic photooxidation are small carbonyls as well as small amounts of alcohols and acids (*4*, *10*, *12*). Jang *et al.* showed that some of the highly volatile carbonylic oxidation products (expected to be mostly in the gas phase) can lead to an increase of SOA mass if mixed with strongly acidic inorganic seed particles (*13*). They proposed condensation and polymerization reactions of carbonyls in the acidic particles as a possible explanation of the observed SOA mass increase. However, their analytical techniques did not allow the actual detection of the proposed polymers. Our reaction chamber measurements show that about 50% of SOA from aromatics oxidation is composed of polymers. This polymerization is a long-term process lasting over more than 20 hours.

The aerosol was generated for measurements described here under controlled conditions in a 27-m^3 Teflon polytetrafluoroethylene bag (Foiltech GmbH, Bremen, Germany) by photooxidation of 1,3,5-trimethylbenzene (TMB), with initial mixing ratios of 20 to 650 parts per billion by volume (ppbv) resulting in maximum particle mass concentrations between 2.7 $\mu g/m^3$ (40 ppbv) and 170 $\mu g/m^3$ (650 ppbv) (*14*). Figure 1 shows a mass spectrum obtained with laser desorption ionization–mass spectrometry (LDI-MS) (*14*) from an SOA sample collected 5 to 7.5 hours after start of the photooxidation. A large number of compounds up to a mass region of about $m/z = 1000$ (where m is the ion mass and z is its charge) is seen. The group of peaks in the range $400 < m/z < 900$ shows highly regular mass differences of m/z of 14, 16, and 18 (Fig. 1, inset). Such a regular structure is typical for polymers, suggesting that polymerization reactions are taking place in the aerosol particles. TMB has a mass of 120 daltons, whereas masses up to $m/z = 900$ become gradually visible with increasing intensity within 7.5 hours after particle nucleation (Fig. 2, A to D). During the whole time, peak intensities changed, whereas the profile remained unchanged.

Measurements of the gas and particle phase with GC-MS and ion chromatography (IC) showed that about 30 small carbonyls and acids are produced as reaction products of TMB. Most of these compounds were previously found by other authors (*15*, *16*). One of the most abundant gas-phase oxidation products of TMB [with a molecular yield of about 0.9 (*15*)] is methylglyoxal, a C_3-dicarbonyl, which is also found in the ambient atmosphere up to ppbv mixing ratios (*17*).

An aqueous solution of glyoxal is primarily composed of hydrated monomers but also contains a significant fraction of dimers and trimers forming acetals (*18*, *19*). Nuclear magnetic resonance (NMR) measurements indicate that the

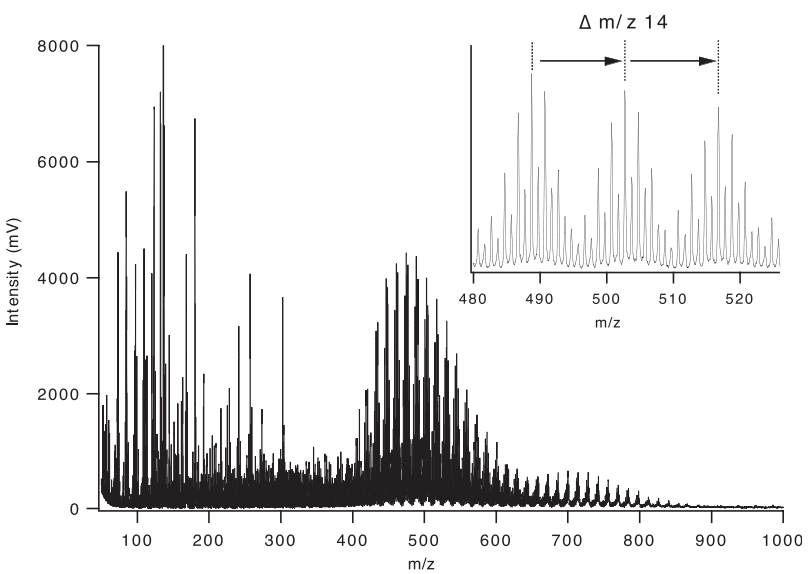

Fig. 1. LDI-MS of secondary organic aerosol resulting from photooxidation of 650 ppbv TMB in the range of $50 < m/z < 1000$. The particles were analyzed without further pretreatment after collection on steel plates using an impactor (*14*). (**Inset**) A detail from $480 < m/z < 525$, showing the repetitive groups with $\Delta m/z$ of 14.

[1]Department of Chemistry and Applied Biosciences, ETH Zurich, 8053 Zurich, Switzerland. [2]Laboratory of Atmospheric Chemistry, Paul Scherrer Institute, 5232 Villigen PSI, Switzerland.

*To whom correspondence should be addressed. E-mail: urs.baltensperger@psi.ch (U. B.); kalberer@org.chem.ethz.ch (M. K.)

equilibrium is shifted to higher acetal polymers with lower water content of the solution. LDI-MS measurements of methylglyoxal showed oligomers up to the nonamer with m/z = 723 (Fig. 2E) (*14*). Several hydrates for each oligomer were detected, with the dihydrate being mostly the prominent peak, confirming the above NMR studies.

An LDI mass spectrum of an equal-mass aqueous solution of methylglyoxal, formaldehyde, 3,5-dimethylbenzaldehyde, and pyruvic acid (all known oxidation products of TMB), a viscous liquid when dried, is shown in Fig. 2F. An oligomer pattern similar to the TMB-SOA is observed in the range of $400 < m/z < 900$ (Fig. 2D). On the basis of the above-mentioned NMR studies and our LDI-MS measurements, Fig. 3 shows the proposed nonradical-induced acetal polymerization with methylglyoxal as the main monomer unit. However, as shown for 3,5-dimethylbenzaldehyde and pyruvic acid, other carbonyls as well as carbonyl-containing acids may also be incorporated into the polymer (*20*). Although no evidence was found in these NMR analyses (*19*, *20*), other nonradical reactions such as aldol condensation reactions could occur in the complex organic mixture of the aerosol.

The repetitive groups of four to five compounds at $400 < m/z < 900$ with mass differences of 14, 16, and 18 (Fig. 1, insert) can be explained with the formation of hydrates ($\Delta m/z$ = 18), the addition of an acid instead of a carbonyl (that is, pyruvic acid instead of methylglyoxal, $\Delta m/z$ = 16), or the incorporation of compounds that have a mass equal to a multiple of 14, 16, or 18 (e.g., formaldehyde with a mass of 30 = 14 + 16). The polymer can be further oxidized within the particle by ultraviolet (UV) light or OH radicals, also resulting in mass increases.

All of the four or five highest peaks of the repetitive groups in this mass range can be explained by linear combinations of these four proposed monomers (methylglyoxal, formaldehyde, 3,5-dimethylbenzaldehyde, and pyruvic acid), which are measured by proton transfer reaction–MS during the full course of the experiment (fig. S2). However, other carbonyls (among them likely also second- and third-generation products) may also be incorporated into these polymers. This explains the similar but not identical mass pattern for the SOA and the surrogate mixture spectra.

The polymer proposed in Fig. 3 has a low carbon-to-oxygen atomic ratio of about 1:1, depending on the degree of oxidation. High-resolution mass spectrometry of the TMB-SOA samples with Fourier-transformed ion cyclotron resonance with a mass accuracy of about 10 parts per million (ppm) supports this hypothesis. Assuming only C, H, and O atoms as constituents, the analyzed peaks (e.g., 463.17, 479.15, or 507.18) have a C:O ratio of 1:0.7 to 1:1.6. All SOA constituents identified so far in the literature were small, up to about 200 daltons (*4*, *10*, *12*). The identification of acetal polymers as a major class of compounds will strengthen the qualitative and quantitative understanding of SOA formation.

A volatility tandem differential mobility analyzer (VTDMA) was used to quantify the polymer fraction (*21*). This technique characterizes the aerosols on the basis of aerosol electrical mobility and thermodynamic behavior. Size reduction of the aerosol due to evaporation at 100°, 150°, and 200°C is detected. The VTDMA particle size selection ranged from 15 to 240 nm depending on the peak evolution of the size distribution.

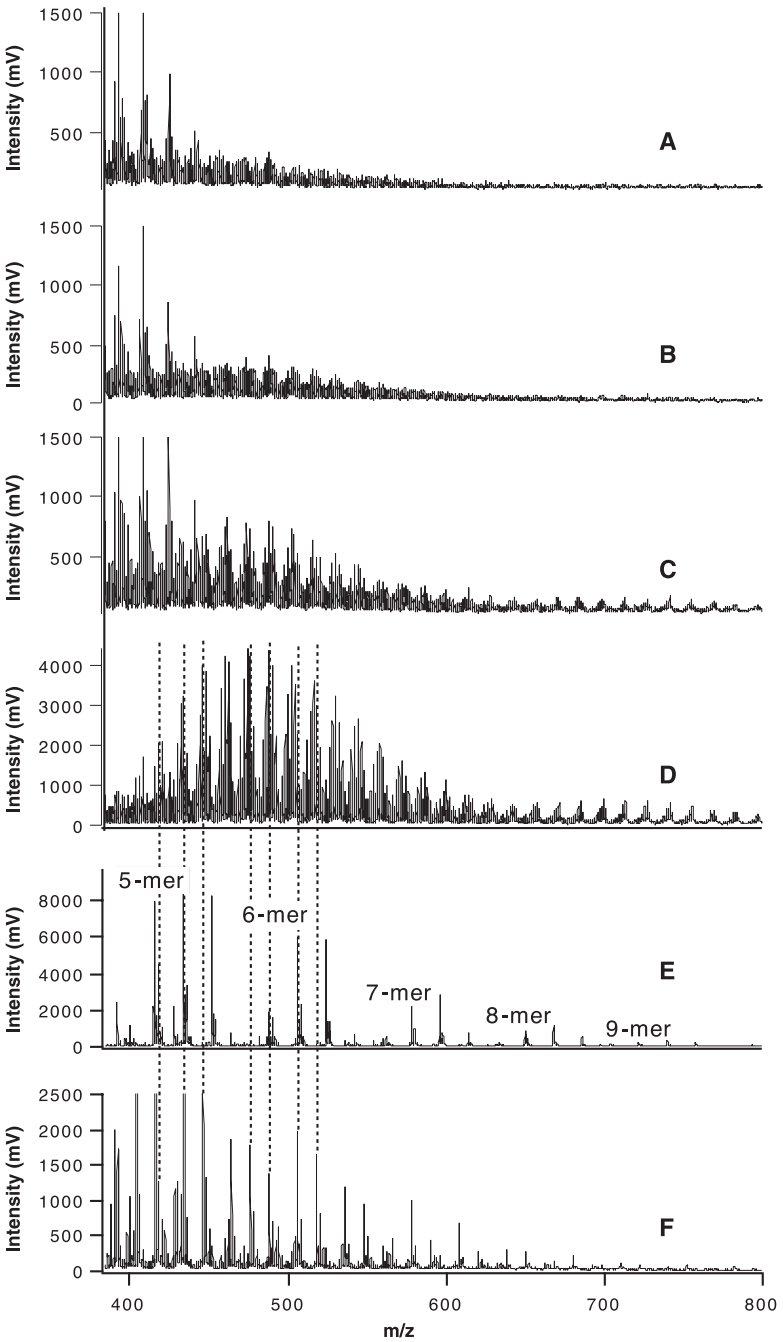

Fig. 2. Time evolution of polymers in SOA from TMB measured with LDI-MS after (**A**) 2.5 hours, (**B**) 3.5 hours, (**C**) 4.5 hours, and (**D**) 6.5 hours. After 2.5 hours of irradiation, only a few peaks are detected at $m/z > 400$ (A). With increasing time, the molecular size distribution shifts to higher masses. After 3.5 hours (B), the polymer structure for $400 < m/z < 600$ becomes visible. Another hour later, the high mass end of the polymer distribution ($600 < m/z < 900$) becomes more visible (C) and the maximum of the polymer mass distribution shifts gradually to higher masses [up to about m/z = 500 after 6.5 hours (D)]. LDI-MS of (**E**) methylglyoxal oligomers and (**F**) a synthetic mixture of methylglyoxal, pyruvic acid, formaldehyde, and 3,5-dimethylbenzaldehyde.

The increase with time in the remaining volume fraction of particles after passing through the VTDMA at the three temperatures is shown in Fig. 4. The high-concentration (650 ppbv TMB, solid symbols) data show that, after about 1 hour of irradiation, the particle volume fraction remaining at 100°C gradually increases from about 30% to more than 85% over the course of 27 hours. Whereas the initial 30% nonvolatile fraction at 100°C is interpreted to be due to low-volatility monomers or small oligomers, the increase over time from 30% to more than 85% is mostly because of polymer formation. Similar trends were measured at 150°C and 200°C. These changes correspond to the temporal evolution of the mass spectra as discussed above.

Preliminary hygroscopicity TDMA measurements indicate no significant increase in hygroscopic growth of the particles after the first 8 hours (with a growth factor of 1.10). This is an additional indication that polymers and not highly oxidized reaction products (i.e., more hygroscopic compounds such as multifunctional acids) are mainly responsible for the increasing low-volatility fraction.

After the initial buildup of the aerosol phase (0 to 5 hours), the aerosol volume (fig. S1) slowly increases. The mixing ratios of most of the ~40 gas phase products (fig. S2) remain constant or decrease slowly after this time (with the exception of the buildup of CO, methanol, and small acids). These small changes in the gas phase are still much greater than the changes observed in the aerosol phase. Assuming 10 monomers to participate in the polymerization, only a few ppbv are needed of each single monomer to build up the polymer (*14*). A change in chemical structure is also observed by infrared spectroscopy, with a continuous broadening of the OH stretch and the C=O bands indicating that these groups get more pronounced over a prolonged time scale (fig. S3) (*14*).

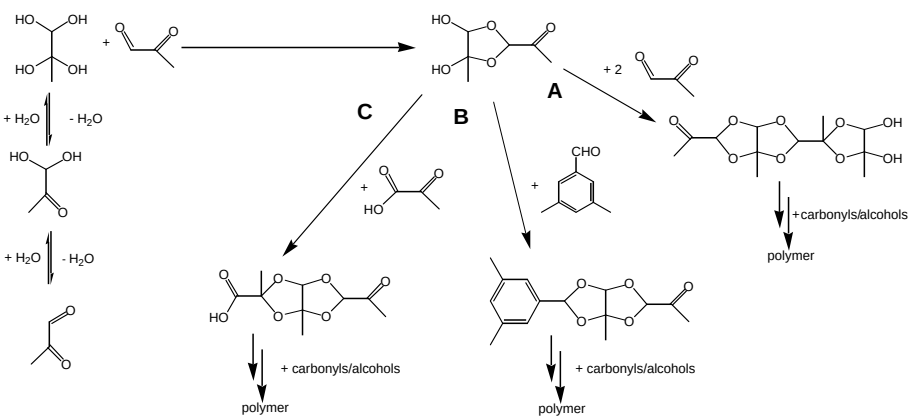

Fig. 3. Chemical structure and formation reactions of the proposed SOA polymer from aromatics oxidation. Acetal polymers are formed from carbonyls and hydrated carbonyls or other alcohols. Route (A) shows a pure methylglyoxal polymer and routes (B) and (C), the incorporation of 3,5-dimethylbenzaldehyde and pyruvic acid, respectively, into the polymer.

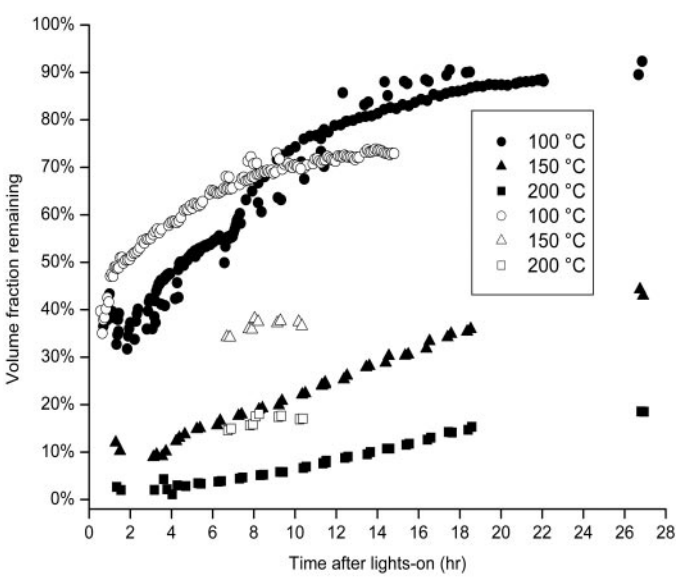

Fig. 4. VTDMA data from eight independent experiments. In contrast to the data at 100°C, the changes at 150°C and 200°C reflect a higher degree of polymerization and correspondingly lower volatility. The solid symbols are high-concentration (650 ppbv TMB and 320 ppbv NO_x) data; open symbols are low-concentration (20 and 40 ppbv TMB and 10 and 20 ppbv NO_x) data. This decrease in volatility is explained with continuing polymerization reaction within the aerosol particle. Polymerization at the lower concentration occurs more rapidly for the first ~4 hours of irradiation; however, after this time the rate is slower than at high concentrations.

The results of experiments, performed with the use of atmospherically relevant initial mixing ratios (open symbols) of 40 and 20 ppbv of TMB (20 and 10 ppbv NO_x, respectively), are also shown in Fig. 4. At these lower concentrations, particles were observed to initially (1 to 9 hours) have higher volume fractions remaining for the same irradiation time. For example, after about 5 hours, the 100°C data have a volume fraction remaining value of 62%, in contrast to a value of 50% for the high concentration data at the same time and temperature. This higher initial polymerization rate could be explained by a higher surface-to-volume ratio of the particles in the low concentration case, resulting in a higher reaction rate for surface-limited processes. However, there are also other possible reasons, like higher acid concentrations in the aerosol (enhancing acid-catalyzed reactions) or higher monomer concentrations in the aerosol (yielding a higher polymerization rate).

In contrast to the experiments of Jang *et al*. (*13*), polymerization proceeds here without preexisting strong acids on seed particles. SOA was formed here by homogeneous nucleation without any seed particles. Thus, the only acids present in the system are formed in the photooxidation of TMB and NO_x. Organic acids belong to the final oxidation products of organic compounds and thus increase over the whole time of the experiments in the gas and the aerosol phase. Organic acids collected after 2 to 6 hours of irradiation and determined by IC (including formic acid, acetic acid, and dicarboxylic acids) amounted to 1.0 equivalents per liter, corresponding to about 7% of the total aerosol mass. In addition, nitric acid was found in appreciable amounts (0.1 mol/l). This compares well with the total H^+ concentration from weak acids of about 1.4 mol/l obtained for an aliquot of the same sample by microtitration (*22*). Acids formed in the photooxidation are thus present in sufficiently high concentrations to catalyze acetal polymerization reactions. These measurements show that polymerization in atmospheric aerosols takes place also without acidic seed particles and in a wide range of atmospheric conditions.

So far, this polymerization has only been shown for TMB photooxidation products. However, methylglyoxal and glyoxal (which also readily polymerizes) are major oxidation products of all other important aromatic compounds in the atmosphere (*23*). In other words, this type of polymer is expected to be formed in substantial amounts from all aromatic precursors. Because aromatics are the main anthropogenic SOA precursors, these polymers are also likely to be found in urban polluted atmospheres. The polymerization observed here continued over more than 20 hours of irradiation. Considering

an average lifetime of tropospheric aerosol of 1 week, one can expect that polymerization reactions occur in an organic aerosol during its entire lifetime, altogether changing its chemical and thermodynamic properties continuously. It is to be expected that polymerizing reactants are diluted in the real atmosphere by preexisting organic material. This may to some extent reduce the polymerization rate; however, further experiments with organic seed particles are required to verify this hypothesis.

In addition, aldehydes are also abundant oxidation products of biogenic terpenes (e.g., pinonealdehyde or norpinonealdehyde). Thus, it is likely that acetal polymers are also formed in rural areas where emissions of aromatics are small. In recent years, many studies tried to correlate ambient measurements of gaseous organic compounds with observed particle nucleation events to identify possible SOA precursors concentrating mostly on low-volatility acids or diacids (*24*). Accordingly, a closer look into compounds such as (di-)aldehydes (which readily polymerize) as potential nucleating agents is suggested.

These findings have a number of implications for SOA modeling. Current models estimating the SOA mass formation assume a thermodynamic equilibrium of gaseous oxidation products and the particle phase (*4*, *6*, *7*). However, the uncertainty in the specific partitioning parameters may result in huge discrepancies. A recent comparison of SOA models found predicted SOA concentrations to vary by a factor of 10 or more, where the partitioning parameters were a key difference (*25*). In other sensitivity studies, reducing the saturation concentrations for all precursors by a factor of 10 increased the predicted SOA mass more than twice, whereas with a fixed equilibrium gas mixing ratio of 2 parts per trillion the total SOA concentration went up by a factor of 3 to 4 (*26*). The latter had been used in early SOA modeling (*27*) and was regarded as an upper-limit estimate for SOA formation. Model results with low vapor pressure will also yield diurnal variations that are more similar to measurements, with the maximum concentration in the afternoon (*28*), whereas high vapor pressure data tend to result in a minimum in the afternoon, when temperature is highest (*29*).

Consequently, modeling studies addressing mechanistic aspects of SOA formation may need to readdress the current assumptions on the basis of the polymerization reactions proposed here. Although the concept of two different vapor pressures for lumped compounds (*4*) might still be applicable, current interpretations of the model parameters might need to be revised. Revised models will result in higher SOA yields, especially at higher temperature and with different temperature dependence. Further experiments are needed to explore the absorption behavior of the high volatility fraction in the polymerizing material. Moreover, it can be expected that these polymerization reactions affect a number of other aerosol properties such as optical parameters, hygroscopic growth, and cloud condensation nuclei potential, which are crucial for the role of aerosols in the global climate system.

References and Notes

1. J. H. Seinfeld, S. N. Pandis, *Atmospheric Chemistry and Physics* (Wiley, New York, 1998).
2. W. F. Rogge, M. A. Mazurek, L. M. Hildemann, G. R. Cass, B. R. T. Simoneit, *Atmos. Environ.* **27A**, 1309 (1993).
3. H.-J. Lim, B. J. Turpin, *Environ. Sci. Technol.* **36**, 4489 (2002).
4. D. R. Cocker, B. T. Mader, M. Kalberer, R. C. Flagan, J. H. Seinfeld, *Atmos. Environ.* **35**, 6073 (2001).
5. M. D. Hurley *et al.*, *Environ. Sci. Technol.* **35**, 1358 (2001).
6. J. R. Odum, T. P. W. Jungkamp, R. J. Griffin, R. C. Flagan, J. H. Seinfeld, *Science* **276**, 96 (1997).
7. J. F. Pankow, *Atmos. Environ.* **28**, 189 (1994).
8. R. J. Griffin, D. R. Cocker, R. C. Flagan, J. H. Seinfeld, *J. Geophys. Res.* **104**, 3555 (1999).
9. W. Dechapanya, A. Eusebi, Y. Kimura, D. T. Allen, *Environ. Sci. Technol.* **37**, 3662 (2003).
10. M. S. Jang, R. M. Kamens, *Environ. Sci. Technol.* **35**, 3626 (2001).
11. A. Holes, A. Eusebi, D. Grosjean, D. T. Allen, *Aerosol Sci. Technol.* **26**, 516 (1997).
12. H. J. L. Forstner, R. C. Flagan, J. H. Seinfeld, *Environ. Sci. Technol.* **31**, 1345 (1997).
13. M. Jang, N. M. Czoschke, S. Lee, R. M. Kamens, *Science* **298**, 814 (2002).
14. Information on materials and methods is available as supporting material on *Science* Online
15. D. F. Smith, T. E. Kleindienst, C. D. McIver, *J. Atmos. Chem.* **34**, 339 (1999).
16. J. Yu, H. E. Jeffries, K. G. Sexton, *Atmos. Environ.* **31**, 2261 (1997).
17. E. Grosjean, D. Grosjean, M. P. Fraser, G. R. Cass, *Environ. Sci. Technol.* **30**, 2687 (1996).
18. E. B. Whipple, *J. Am. Chem. Soc.* **92**, 7183 (1970).
19. F. Chastrette, C. Bracoud, M. Chastrette, G. Mattioda, Y. Christidis, *Bull. Soc. Chim. Fr. II-CH* **1-2**, 33 (1983).
20. F. Chastrette, C. Bracoud, M. Chastrette, G. Mattioda, Y. Christidis, *Bull. Soc. Chim. Fr.* **1**, 66 (1985).
21. D. J. Rader, P. H. McMurry, *J. Aerosol Sci.* **17**, 771 (1986).
22. Titration was performed from a 1:1 (water:acetone) extract with 0.01 M NaOH with a 809 Titrando (Methrom, Herisau, Switzerland).
23. J. Calvert *et al.*, *Mechanisms of Atmospheric Oxidation of Aromatic Hydrocarbons* (Oxford Univ. Press, Oxford, 2002).
24. T. Hoffmann, R. Bandur, U. Marggraf, M. Linscheid, *J. Geophys. Res.* **103**, 25569 (1998).
25. B. K. Pun, S Y. Wu, C. Seigneur, J. H. Seinfeld, R. J. Griffin, S. N. Pandis, *Environ. Sci. Technol.* **37**, 3647 (2003).
26. B. Koo, A. S. Ansari, S. N. Pandis, *Atmos. Environ.* **37**, 4757 (2003).
27. S. N. Pandis, R. A. Harley, G. R. Cass, J. H. Seinfeld, *Atmos. Environ.* **26A**, 2269 (1992).
28. B. J. Turpin, J. J. Huntzicker, *Atmos. Environ.* **25A**, 207 (1991).
29. P. E. Sheehan, F. M. Bowman, *Environ. Sci. Technol.* **35**, 2129 (2001).

30. We thank R. Richter and M. Furger for their help in the smog chamber construction and instrument development and M. Reifler, Metrohm, Herisau, for performing the acid titrations. This work was supported by the Swiss National Science Foundation.

Supporting Online Material

www.sciencemag.org/cgi/content/full/303/5664/1659/DC1
Materials and Methods
Figs. S1 to S3
References

3 October 2003; accepted 12 February 2004

Induction of Protective IgA by Intestinal Dendritic Cells Carrying Commensal Bacteria

Andrew J. Macpherson* and Therese Uhr

The enormous number of commensal bacteria in the lower intestine of vertebrates share abundant molecular patterns used for innate immune recognition of pathogenic bacteria. We show that, even though commensals are rapidly killed by macrophages, intestinal dendritic cells (DCs) can retain small numbers of live commensals for several days. This allows DCs to selectively induce IgA, which helps protect against mucosal penetration by commensals. The commensal-loaded DCs are restricted to the mucosal immune compartment by the mesenteric lymph nodes, which ensures that immune responses to commensal bacteria are induced locally, without potentially damaging systemic immune responses.

Mammals and other vertebrates coexist with an extremely dense and diverse microflora of nonpathogenic bacteria in the lower intestine, which salvage the energy of otherwise indigestible dietary carbohydrates and compete with the growth of pathogenic organisms. Although this mutualism can break down in individuals with inflammatory bowel disease, coevolution of commensals and their hosts has ensured that inflammatory intestinal immunopathology is relatively rare.

Comparisons between experimental germ-free animals and those containing

Institute of Experimental Immunology, Universitätsspital, CH8091 Zürich, Switzerland.

*To whom correspondence should be addressed. E-mail: amacpher@pathol.unizh.ch